*Int. J. Chem. Sci.: 13(3), 2015, 1345-1356*
*ISSN 0972-768X*
*www.sadgurupublications.com*

# SYNTHESIS OF HIGH SURFACE AREA MICROPOROUS SPIRO-POLYMER FOR GREEN CHEMISTRY APPLICATIONS

**FADI IBRAHIM***

Department of Chemistry, Abdul Latif Thanian Al-Ghanim School Kuwait,
ARDEIA, Part 6, Fst Str, KUWAIT

## ABSTRACT

Three anthracene microporous polymers (AMPs) bridged by imide links were successfully prepared by conventional nucleophilic substitution reaction between different 9,10-dihydro-9,10-ethanoanthracenes and 2,3,5,6-tetrachlorophalonitrile (instead of fluoro-monomer)[1,2]. AMPs display a BET surface area in the range of 711-796 $m^2$ $g^{-1}$, and adsorb reach to 1.70 wt.% $H_2$ at 1.09 bar/77 K. The enhanced microporosity, in comparison to other organic microporous polymers originates from the macromolecular shape of framework, as dictated by the anthracene units, which helps to reduce intermolecular contact between the extended planar struts of the rigid framework. The impressive hydrogen adsorption capture of these materials verified by Horvath-Kawazoe (HK) and NLDFT analyses of low-pressure nitrogen adsorption data, which expected to be use in transportation as a source of green chemistry.

**Key words**: Anthracene, Microporous, AMP, Polymer.

## INTRODUCTION

The preparation of purely organic microporous polymers without the assistance of molecular template is becoming a fast developing area in nonmaterial's research and many approaches have been used to develop various insoluble network organic microporous polymers such as hyper cross-linked polymers (HCP), triptycene-based PIM (Trip-PIM)[3], conjugated microporous polymers (CMP)[4], organic framework polymer (OFP)[5], porous organic polymers (POP)[6] and microporous polyimide networks[7] with high specific surface. The microporosity is maintained by a robust network of covalent bonds, further complemented by rigid framework structure. Generally non-network polymers pack space efficiently. However, it has been long understood that some polymers can possess large

*Author for correspondence; E-mail: fed_ooo@yahoo.com

amount of free void volume. It is important to note that if there is a certain amount of free volume, voids would be interconnected, and the polymer will therefore behave as a microporous material even without a network structure. This kind of microporous polymer could be soluble to facilitate easy solution-based processing, which can't be achieved in other microporous materials.

As a result, they have attracted good acceptance as outstanding membrane in gas separation, gas storage, adsorption of small molecules and heterogeneous catalysis[8]. So, it is of great interest to synthesize highly soluble porous polymers using the established dioxane-forming polymerization reaction between appropriate chlorine-containing monomers and the commercially available aromatic tetrol. The porous properties mainly due to the architectural features of the used monomers, which defines the microporosity. The combined features: high rigidity arising from dioxane linkages and the randomly contorted structure due to either a spiro-centre or a non-planar architecture, represent a prerequisite to induce space inefficient packing producing a large amount of interconnected free volume.

The most outstanding representation for this kind of materials are the polymers of intrinsic microporosity (PIMs) developed by McKeown and Budd et al.[9] with high surface areas in the range of 500-900 $m^2/g$. Typical example is PIM-1, prepared as a soluble polymer from the dioxane forming reaction between 5,5',6,6'-tetrahydroxy-3,3,3',3'-tetramethylspirobisindane and 4-dicyanotetraflurobenzene. The objective of the paper is to develop a new high surface area of soluble organic polymers, to study its potential utility in hydrogen, nitrogen storage and its related applications. Great interests in soluble, microporous polyimides[10] due to there are much easier to process than crosslinking polymers. However, only a very limited number of microporous, soluble polymers are known up to now.[11-15] This can be related to the high polymerization difficulty, which are posed onto polymer architecture in order to provide both high free volume and resistance against pore collapse. This paper investigates the influence of the molecular structure, reaction temperature, $K_2CO_3$ and solvent effects on polymerization. It is important to focuses on the impact of polymer backbone architecture (kink as TTSBI monomer, angle, and monomer length as SI-(1-7)-4F, etc). Condensation of these monomers with TTSBI allows a tuning of the overall polymer flexibility and the spacing between the kinks along the polymer chain.

## Polyimide chain-chain interactions

Fig. 1 shows the idealized form of such an interaction between the dianhydride and diamine groups (increased interchain attractive forces due to such interactions) and AMP type of idealized chain-chain interaction. It was also proposed that the presence of any

bridging group in the dianhydride had a strong influence on the glass transition as it changed its electron affinity and hence promoted the possibility of CTC formation.

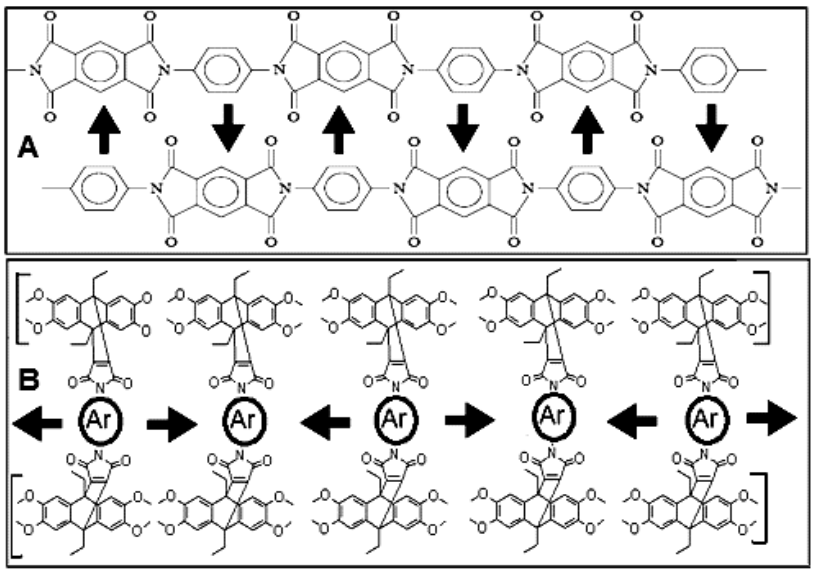


**Fig. 1: (A) Idealized charge transfer complex formation in dianhydrides and (B) AMP type of idealized chain-chain interaction**

Such chain packing models have also been utilized to qualitatively explain the predominating effect of any bridging groups present in the dianhydride, which then may disrupt the packing arrangement by inhibiting the carbonyl-carbonyl dipolar attractions. The presence of such bridging groups in the diamine has been proposed to only reduce the packing density and thus exerts lesser influence on the final Tg. While such explanations provide some degree of qualitative explanation of Tg behavior, they cannot be utilized for any convenient quantification to predict the Tg. Although such ideal chain-chain interactions have been hypothesized, the structural arrangements within any polyimide should be governed by minimum energy conformations.

## EXPERIMENTAL

### Materials and methods

All the chemicals were of reagent grade purity and used without further purification. The dry solvent Dimethylformamide (DMF) with water content less than 0.005% was purchased from Aldrich Co. The finely grounded anhydrous potassium carbonate was used after further drying at 200$^{o}$C. $^{1}$H-NMR spectrum (400 MHz) of monomers were recorded on

a Bruker DPX 400 spectrometer using $CDCl_3$ as the solvent and tetramethylsilane as the internal standard. Solid state $^{13}C$-NMR measurement was carried out on a Bruker Avance 300 spectrometer equipped with a cross polarization magic angle spinning (CP/MAS) probe and a fully automated pneumatic unit for sample spinning. The specific surface area was calculated using the Brunauer-Emmet-Teller (BET) equation. The micropore area was calculated using *t*-plot method. The pore size distributions were calculated from the adsorption isotherm using the Horvath-Kawazoe (H-K) and Nonlocal Density Functional (NLDFT) calculations. The heats of adsorption for $H_2$ was calculated using the ASAP 2020 software (Micromeritics, Norcross, GA).

## Synthesis of AM-8OH monomers

The octahydroxy-monomer (f) prepared in multistep starting from the reaction between the propanaldehyde and veratrole in 84% $H_2SO_4$, which result 9,10-dialkyl-2,3,6,7-tetramethoxyanthracene (a), followed by adding of dimethlacetylenedicarboxylate to (a) to produce (b) as shown in **Scheme 1**.

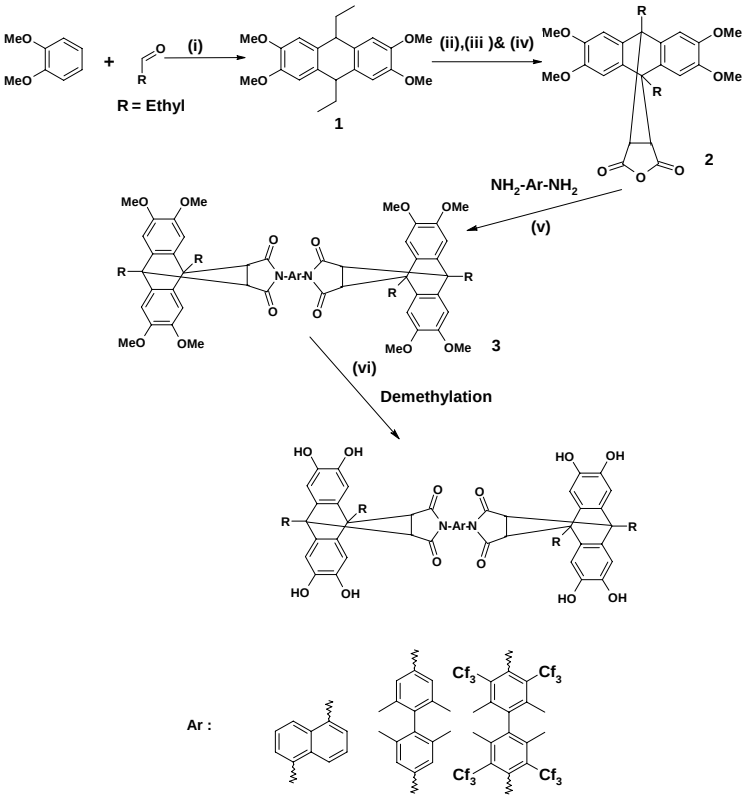


**Scheme 1: Synthetic pathway toward the octahydroxy-monomers**

**Reagents and conditions:** (i) dimethlacetylenedicarboxylate, 84% sulfuric acid, 5$^{o}$C; (ii) 210$^{o}$C for 20 min; (iii) ethanol-water 100$^{o}$C for 3 hr; (iv) reflux in acetic anhydride for 3 hr; (v) reflux in acetic acid for 24 hr; (vi) $BBr_3$, and $CH_2Cl_2$ at 5$^{o}$C for 3 hr.

## Synthesis of AMPs

Microporous rigid polymers (AMPs) based on 9,10-dihydro-9,10-ethanoanthracenes monomers bridged by imide links was synthesized efficiently by the double aromatic nucleophilic substitution reaction as shown in **Scheme 2**. This nucleophilic substitution reaction apply dioxane,[14] forming reaction between the corresponding octahydroxy monomers and tetrachluoro-terphthalonitrile (instead of tetrafluoro-terphthalonitrile)[1] in dry DMF and 100$^{o}$C.

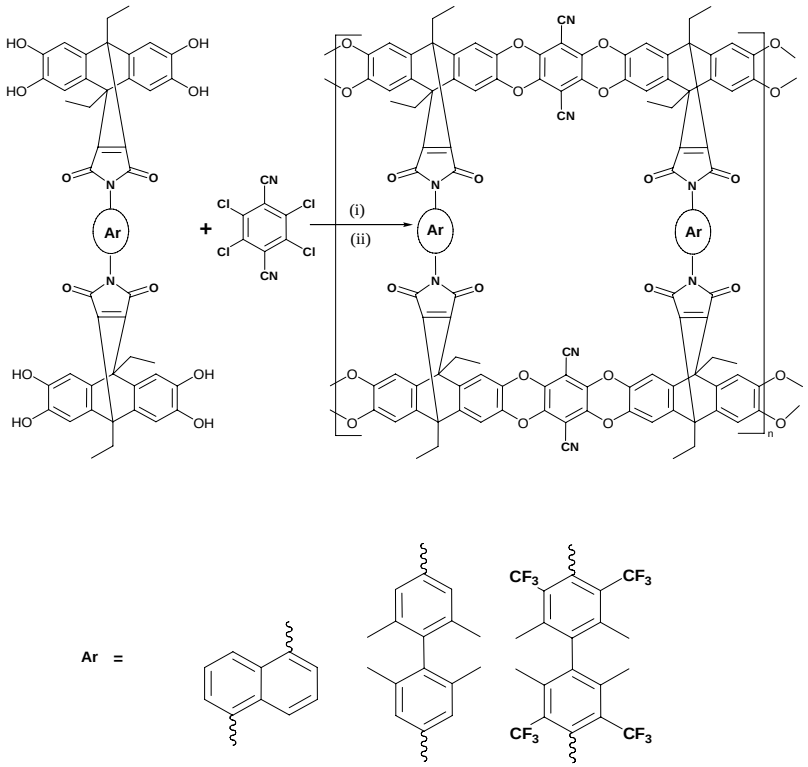


**Scheme 2: Synthetic pathway toward the polyamide network AMP (5-7)s. Reagent and conditions: (i) $K_2CO_3$, and DMF (ii) 100$^{o}$C for 48 hr**

The network polymer was washed with a variety of organic solvents and dried under vacuum. The anthracene based monomers (AMP$^{5-7}$) were prepared in good yield by the

straight forward one step imidisation reaction between corresponding anhydride and different amines in refluxing acetic acid. The proposed structure and purity of the obtained monomers were confirmed by routinely spectroscopic techniques as well as elemental analysis. The polymers AMP-[5-7] were synthesized by the dibenzodioxane formation reaction between the tetrol, and tetra-chloroterephthalonitrile in dry DMF as illustrated in Scheme 1. The structures of all prepared AMPs were characterized by FT-IR, solid state $^{13}C$ NMR spectroscopy and elemental analysis. All materials retained its characteristic stretching bands related to the imide groups (C=O symmetric and asymmetric stretching in the range of 1722-1792). Moreover, it is clear from the spectrum that the base catalyzed polymerization condition does not make any destruction in the imide units. The $^{13}C$ NMR spectra of the AMPs were fully consistent with their proposed structures. The signals originating from the hydroxyl groups of tetrol were disappeared, suggesting that the reaction was carried out completely through dibenzodioxane formation. The broad aromatic and aliphatic signals of AMPs were enough to confirm the formation of high molecular weight polymers.

The thermal properties were evaluated by TGA and DSC. The decomposition temperatures were also very high; where a 5-10% initial loss around 400$^{o}$C, were observed, corresponding to the vaporation of the residual solvents, which has been identified as the entrapped solvents in the micropores used for processing the sample. The good thermal stability can be attributed to its double stranded structures. In DSC analysis no melting ($T_m$) and glass transition ($T_g$) was observed. Wide Angle X-ray Diffraction (WAXD) analysis of the AMPs was conducted to display no crystalline peaks and revealed that all the prepared materials were amorphous.

**Structure-property relationship**

Different spacers have been employed in order to evaluate the structure feature on surface area. The anthracene groups as thermally and oxidatively stable, rigid moiety can improve physical properties such as enhanced thermal stability, increased chain stiffness, and decreased crystallinity.[15] However, for AMP-6 and 7 there is very highly restricted rotation about the imide bond linkages, giving rigidity to the polymer. In AMP-5, there is potentially more flexibility in the backbone, but the hexafluoroisopropylidene unit provides a kink in the chain and may be regarded as an additional site of contortion. The unique shape of the anthracene unit lead to a rigid network structure composed of nanoporous frameworks. The molecular structures of these PIM-polyimides have features of the spiro-center providing a site of contortion as well as having conventional imide linkages, this results a very highly restricted rotation about these bonds, giving rigidity to the polymer. The faces of

the ribbonlike "struts" between the anthracenes are oriented nearly perpendicular to the plane of the macromolecular growth. This arrangement blocks face-to-face association between these planar struts, leading to greater IM. For the attainment of microporosity in network polymers, it appears that the requirement for the prevention of rotation about single bonds is unperturbed, presumably due to the network itself preventing structural rearrangement that could result in a collapse of the porous structure. Hence, the formation of rigid amorphous network polymers using anthracene monomer is compatible with obtaining highly microporous materials. Perhaps the clearest demonstration of IM is found for well defined rigid oligomers containing triptycenes as the concave unit. An interesting structure-property relationship is evident for these materials in that the longer the linear struts between the branch points, the lower is the porosity. And is likely related to a larger number of bonds with rotational freedom, which will reduce IM.[10]

## Nitrogen adsorption analysis

Nitrogen adsorption measurements of AMPs where measured, for example, the BET surface area of AMPs is relatively high, which is higher than the Trip-PIM[16] but less than the HCPs[17] as shown in Fig. 2.

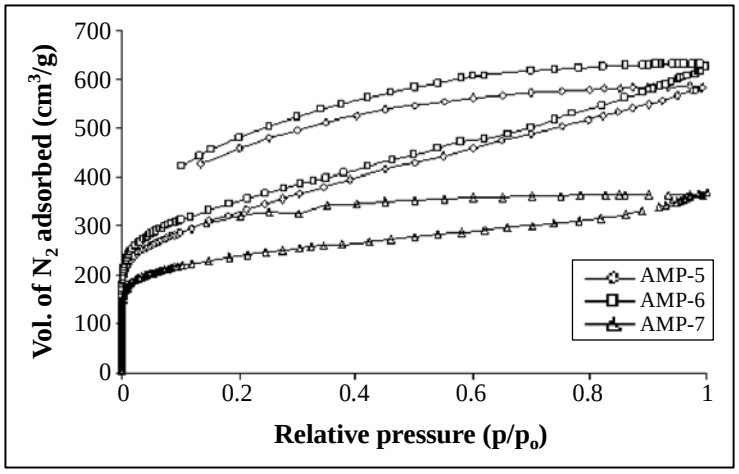


**Fig. 2: Nitrogen adsorption/desorption isotherm at 77 K for AMPs**

Adsorption increased gradually as the pressure was increased. The isotherms are fully reversible and exhibit a sharp rise at low pressure region, which is consistent with the physisorption of hydrogen on a microporous material. All the prepared AMPs show similar behaviors in their isotherm with a significant uptake at two different temperatures (Table 1).

The adsorption/ desorption isotherms clearly exhibit pronounced hysteresis up to low partial pressure, which is typically observed for microporous materials. Nitrogen uptake increases in the sequence AMP-5 < AMP-6 < AMP-7, this is reflected in the results of analysis by the (BET) method, which gave apparent surface areas of 750, 711, and 796 $m^2/g$, respectively.

**Table 1: [a]BET surface area of AMP (5-7)s calculated from nitrogen adsorption isotherm. The number in the parathesis is the micropore surface area calculated using the *t*-plot analysis. $PV_{micro}$ is the micropore volume. [b]Surface area calculated from the $H_2$ adsorption isotherm using Langmuir equation at 77 K and 87 K**

| PIMs | $SA_{BET}$ $(m^2/g)^a$ | $PV_{micro}$ $(cm^3/g)$ | HK/NLDF Tpore width (Å) | $SA_{LAN}$ $(m^2/g)^b$ (77 K/87 K) | $H_2$ (wt.%) at 1.13 bar (77 K/87 K) | $Q_{st}$ (kJ/mole) |
|---|---|---|---|---|---|---|
| AMP-5 | 750 (626) | 0.65 | 5.56/6.29 | 663/523 | 1.59/1.23 | 7.19 |
| AMP-6 | 711 (615) | 0.48 | 5.43/6.64 | 343/275 | 1.70/1.3 | 6.99 |
| AMP-7 | 796 (695) | 0.51 | 5.43/6.64 | 343/275 | 1.52/0.63 | 6.99 |

## Hydrogen adsorption

The main task is finding the potential of the prepared materials in storing considerable amount of hydrogen. For example, the hydrogen storage quantities for AMP-5 in a pressure range 0-100 bar (Fig. 3).

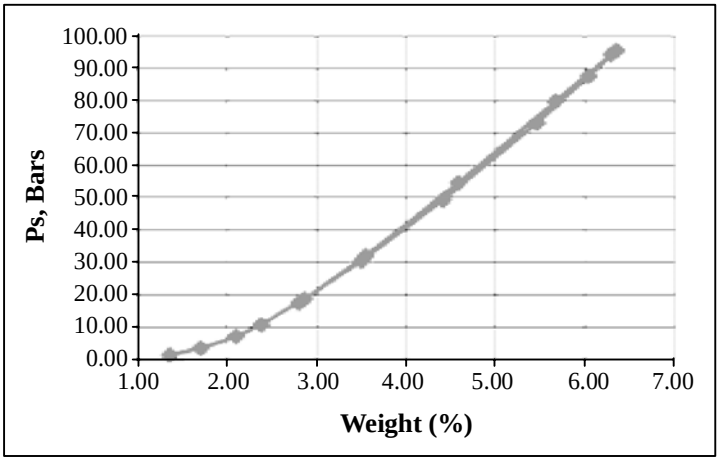


**Fig. 3: High pressure $H_2$ adsorption capacity of AMP-5 (0-100 bar)**

The Langmuir isotherm theory assumes monolayer coverage of adsorbate over a homogenous adsorbent surface of equal energy. The isosteric heat of adsorption, (Qst), for dihydrogen molecules on all samples was calculated from the adsorption isotherms at 77 and 87 K as shown in Fig. 4. The chemical nature of the accessable surfaces and morphology of the pores have thus to be tuned to enable a high adsorption enthalpy. It has been already known that microstructure had a deep impact on hydrogen uptake, which is further influenced by the geometry of the building units. So materials containing high electron rich sites were found to increase the hydrogen adsorption enthalpy. The combination of microporosity and chemical functionality of these AMPs are very promising for applications in the air purification, or separation. As compared to MOFs and similar metal containing porous structures, the concept of preparing hydro-thermally stable AMPs having organic spacers along with predefined functionality allows them to extend in many adsorption applications. In order to attain good storage capacity, it will be necessary to design materials with greater accessible surface area and microporosity. The hydrogen adsorption isotherm measured at 77 K and 87 K and the calculations involve the Langmuir equation and *t*-plot analysis. This methodology avoids the problem of over counting the nanopores that is associated with the specific surface area measured by nitrogen adsorption. Fig. 4 shows the hydrogen adsorption/desorption isotherms of AMP-6.

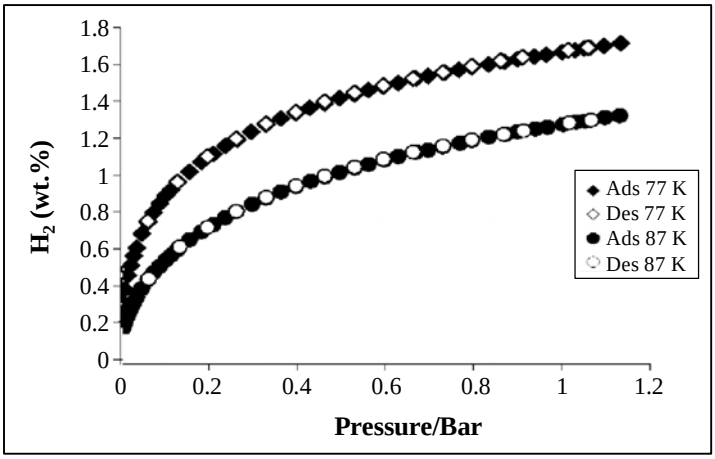


**Fig. 4: Adsorption/desorption isotherms at 77 and 87 K for AMP-6**

In addition, the adsorption is completely reversible and there is no significant hysteresis, which can be correlated with the physisorption of hydrogen on a microporous material. The repeatability of the hydrogen adsorption was also checked and found to be

constant even after the repeated cycles. The shape of the isotherm indicates that adsorption has not reached saturation and further significant hydrogen uptake could occur at higher pressures. The framework OFP-6 afforded a hydrogen storage capacity of 1.70 wt.% at 1 bar and 87 K, which is comparable with the other reported microporous polymers. However, at 77 bars AMP-7 adsorbs nearly 1.55 wt.% by weight of material.

**Pore size distribution**

**Synthesis of AMP-7**

To a solution of octahdroxy-anthracene (0.2 g, 0.21 mmol) and 2,3,5,6-tetrachlorophalonitrile (0.08 g, 0.43 mmol) in dry DMF (40 mL), $K_2CO_3$ (0.35 g, 2.52 mmol) was added and heated to 100$^o$C for 48 hr. Then, the reaction mixture was allowed to cool and precipitated in acidified water. The precipitate was filtered off and washed with deionised water and then with methanol. The purification was done by washed repeatedly with THF and methanol. The resulting AMP-**7** is brown solid and dried in vacuum at 80$^o$C for 12 hrs (yield 80%).

Yield 85%; m.p. > 300$^o$C; MS (EI): m/z (%) 1851 ($M^+$). IR/cm$^{-1}$ (KBr): 1788 (asym C=O, str), 1722 (sym C=O, str), 1366 (C-N, str), 744 (imide ring deformation). $^{13}$C NMR (100 MHz): 169.7, 148.7, 145.3, 142.8, 141.5, 139.5, 138.2, 128.8, 121.6, 123.8, 115.8, 115.2, 104.6, 109.2, 55.8, 55.5, 42.9, 39.6, 15.5, 10.3, 8.6. CHN Calculated for $C_{105}H_{80}F_6N_{10}O_{16}$ (1851): C 68.02; H, 4.32; N, 7.56. Found: C, 67.70; H, 4.21, N, 7.22. BET surface area = 796 m$^2$/g; total pore volume = 0.51 cm$^3$/g.

## ACKNOWLEDGMENT

I'm grateful for the facilities provided by ANALAB, College of Graduate Studies in Kuwait University.

## CONCLUSION

Anthracene-based microporous polymers bridged by imide links (AMPs) was synthesized efficiently by the dioxane forming reactions using cheaper chlorinated monomer instead of fluorinated. AMPs display a BET surface area reach to 796 m$^2$ g$^{-1}$, and reversibly adsorb reach to 1.70 wt.% $H_2$ at 1.13 bar 77 K. The isoteric heat of adsorption about 7.4 kJ/mole. The enhanced microporosity, in comparison to other organic microporous polymers, originates from the macromolecular shape of the framework, as dictated by the triptycene units.

## REFERENCES


1. S. Makhseed and J. Samuel, J. Mater. Chem. A, **1**, 13004-13010 (2013).
2. Fadi Ibrahim, Elixir Nanocomposite Materials, **62**, 17542-17548 (2013).
3. B. S. Ghanem, N. B. McKeown, K. D. M. Harris, Z. Pan, P. M. Budd, A. Butler, J. Selbie, D. Book and A. Walton, Chem. Commun., 67-69 (2007).
4. J. X. Jiang, F. Su, A. Trewin, C. D. Wood, N. L. Campbell, H. Niu, C. Dickinson, A. Y. Ganin, M. J. Rosseinsky, Y. Z. Khimyak and A. I. Cooper, Angew Chem. Int. Ed., **44**, 8574-8578 (2007).
5. S. Makhseed and Samuel, J. Chem. Commun., 4342-4344 (2008).
6. S. Yuan, B. Dorney, D. White, S. Kirklin, P. Zapol, L. Yu and Liu, Di-J. Chem. Commun., **46**, 4547-4549 (2010).
7. Z. Wang, B. Zhang, H. Yu, L. Sun, C. Jiao and W. Liu, Chem. Commun., **46**, 7730-7732 (2010).
8. N. B. McKeown and P. M. Budd, Chem. Soc. Rev., **35**, 675-683 (2006).
9. (a) P. M. Budd, B. S. Ghanem, S. Makhseed, N. B. Mckeown, K. Msayib, C. E. Tattershall and D. Wang, Chem. Commun., **2**, 230-231 (2004).

   (b) P. M. Budd, E. S. Elabas, B. S. Ghanem, S. Makhseed, N. B. McKeown, K. J. Msayib, C. E. Tattershall and D. Wang, Adv. Mater., **16**, 456-459 (2004).

   (c) N. B. McKeown, P. M. Budd, K. Msayib, B. S. Ghanem, H. J. Kingston, C. E. Tattershall, S. Makhseed, K. J. Reynolds and D. Fritsch, Chem.- A European J., **11**, 2610-2620 (2005).
10. Yongli Mi. Takuji Hirose, J. Polymer Res., **3**, 11-19 (1996).
11. Y.H. Kim, H. S. Kim, S. K. Kwon. Macromolecules, , 38, 7950–7956 (2005).
12. J.Li, J. Kato, K. Kudo, S. Shiraishi. Macromol. Chem. Phys., , 201, 2289–2297 (2000).
13. Yuan H., Jui-Ming Y., Shir-Joe L., Yen-P C. Acta Materialia, , 52, 475-486 (2004).
14. Z. M. Qiu, J. H. Wang, Q. Y. Zhang, S. B. Zhang, M. X. Ding and L. X. Gao, Polymer, **47**, 8444-8452 (2006).
15. Y.Tsuda, T. Yoshida and T. Kakoi, Polymer, **38**, 88-90 (2006).
16. J. X. Jiang, Cooper A, Topics Curr. Chem., **293**, 1-33 (2010).

17. D. Hofman, J. Ulbrich, D. Fritsch and D. Paul., Polymer, **37**, 4773-4785 (1996).

18. H. S. Kim, Y. H. Kim, S. K. Ahn and S. K. Kwon, Macromolecules, **36**, 2327-2332 (2003).

19. Yongli Mi. Takuji Hirose, J. Polymer Res., **3**, 11-19 (1996).

*Revised : 11.08.2015* *Accepted : 14.08.2015*